Bioorganic Chemistry 92 (2019) 103191

Contents lists available at ScienceDirect

Bioorganic Chemistry

journal homepage: www.elsevier.com/locate/bioorg

# Novel conjugates with dual suppression of glutathione S-transferases and tryptophan-2,3-dioxygenase activities for improving hepatocellular carcinoma therapy

Shixian Hua, Xinyi Wang, Feihong Chen*, Shaohua Gou*

*Jiangsu Province Hi-Tech Key Laboratory for Biomedical Research, Southeast University, Nanjing 211189, China*
*Pharmaceutical Research Center and School of Chemistry and Chemical Engineering, Southeast University, Nanjing 211189, China*

ARTICLE INFO

*Keywords:*
Glutathione S-transferase
Anticancer
Tryptophan-2,3-dioxygenase
Chemo-immunotherapy
Hepatocellular carcinoma

ABSTRACT

Tryptophan-2,3-dioxygenase (TDO) is an immune checkpoint enzyme expressed in human tumors and involved in immune evasion and tumor tolerance. While glutathione S-transferases (GSTs) are pharmacological targets for several cancer. Here we demonstrated the utility of NBDHEX (GSTs inhibitor) and TDO inhibitor by the combinatorial linker design. Two novel conjugates with different linkers were prepared to reverse tumor immune suppression. The conjugates displayed significant antitumor activity against TDO and GSTs expression of HepG2 cancer cells. Further study indicated that compound **4** could induce higher apoptotic effect than its mother compounds via a mitochondrial-dependent pathway, simultaneously more effective to inhibit TDO and GSTs protein expression. Further study indicated that **4** could decrease the production of kynurenine and deactivate aryl hydrocarbon receptor (AHR), leading to $CD3^+$ *T*-cell activation and proliferation to involve in antitumor immune response.

## 1. Introduction

Liver cancer, the fourth leading cause of cancer death and the sixth most commonly diagnosed cancer in the world, which has no effective strategy to cure, particularly in the later stage of liver cancer [1,2]. According to the records, about 841,000 new Liver cancer cases and 782,000 deaths annually, particularly, the liver cancer rates of mortality ranks second for males [2]. Hepatocellular carcinoma (HCC) is the most common types of primary liver cancers and accounts for about 90% rate of all primary hepatic malignancy cases [3,4]. Furthermore, the survival rate of HCC is very low (about 10%), owing to the high morbidity rate, insufficient diagnosis strategies and disappointing drug development [5–7]. Up to now, the new therapeutic drugs development of HCC is difficult due to the complexity of liver microenvironment and the inexplicable pathological mechanisms of HCC [5,7], particularly, some clinical drugs were successful in phase I/II trials, but failed in phase III trials [8]. Hence, the development of such an effective therapeutic drug for HCC is still a nascent area.

Recently, as a drug target in cancer treatment, glutathione S-transferase (GSTs) have been invoked reconsiderable interest of scientists. The superfamily of GSTs, belong to intracellular dimeric enzymes, which are composed of multifunctional proteins widely distributed throughout mammalian systems and subdivided in about eight gene-independent classes (Alpha, Pi, Mu, Theta, Zeta, Omega, Sigma, and Kappa) [9–16]. GSTs can catalyze the conjugation of the cellular nucleophile GSH with a wide range of electrophilic carcinogens, drugs, toxins, simultaneously producing oxidative stress [17]. Especially, as overexpressed in many cancer cell lines (including cancers of the lung, colon, kidney, ovary and liver) [18,19], GSTs isoenzymes catalyze the conjugation of GSH with specific antitumor agents, prevent antitumor drugs inducing damage vital cellular nucleophiles, lead to increased cancer cells survival and enhanced resistance to chemotherapy [20,21]. Particularly, the acidic form of glutathione S-transferases may be as a hepatic tumor marker [22]. Thus, in combination with GSTs inhibitors is promising to modulate the efficacy of anticancer drugs.

Immune checkpoint inhibitors can involve in *T*-cell-mediated antitumor immune response via several immune checkpoints of biological functions, signaling pathways, and expression levels in tumors [23–26]. Tryptophan 2,3-dioxygenase (TDO), one of immune checkpoints, which is an important negative feedback enzyme encoded by *TDO2* gene and induced by glucocorticoids, tryptophan(Kyp) and kynurenine (Kyn) [27,28]. It is known that TDO mainly expressed in the liver where is its first characterized [28,29]. Similar to indoleamine 2,3-dioxygenase (IDO), TDO can catalyze tryptophan to produce bioactive metabolites

* Corresponding author at: Pharmaceutical Research Center and School of Chemistry and Chemical Engineering, Southeast University, Nanjing 211189, China.
*E-mail addresses:* 101011844@seu.edu.cn (F. Chen), sgou@seu.edu.cn (S. Gou).

https://doi.org/10.1016/j.bioorg.2019.103191
Received 7 February 2019; Received in revised form 1 July 2019; Accepted 9 August 2019
Available online 10 August 2019
0045-2068/ 

including kynurenine along the first and rate-limiting step of the kynurenine pathway, which leading to T cells anergy or apoptosis and tumor tolerance for immune system via depleting tryptophan levels and accumulating its bioactive metabolites [27,30,31]. Hence, inhibition of TDO can reactivate the immune system and reverse tumor-associated immune resistance to kill cancer cells [27–32].

The clinical data provided strong evidence to demonstrate that immune-based therapies are promising for the treatment of HCC, especially in combination with standard chemotherapy [33–35]. Herein, we present an immuno-chemotherapeutic strategy composed of a known TDO inhibitor (**1**, mTDO $IC_{50}$ = 1 μM) [27] and a glutathione S-transferase inhibitor (NBDHEX) bridged by a linker. NBDHEX, a very efficient inhibitor of GSTP1-1 and GSTM2-2, has emerged as an anticancer drug by inhibiting the catalytic activity of GSTs [36,37]. A key point of our strategy is expected to take advantage of immuno-chemotherapeutic to treat HCC.

## 2. Results and discussion

### 2.1. Chemistry

The synthetic method of the targeted compounds and their chemical structures were showed in Scheme 1. NBDHEX and TDO inhibitor **1** were obtained according to the literature reported procedures [16,28]. Compounds **2** and **3**, the derivates of compound **1**, were achieved by treatment of **1** with succinic anhydride or glutaric anhydride in the presence of piperidine and $Et_3N$. The synthesis of the targeted compounds (**4** and **5**) were performed by the formation of ester bond between NBDHEX and TDO inhibitor derivatives (**2** or **3**) using EDCI/DMAP. The chemical structures of all compounds were confirmed by $^1H$ NMR, $^{13}C$ NMR and high resolution mass spectroscopy (HR-MS) (Supporting Information Figs. S1–S6).

### 2.2. Biological evaluations

#### 2.2.1. In vitro cytotoxicity assay

The *in vitro* cytotoxic potency of compounds **4** and **5** were investigated by using MTT assay against four cancer cell lines including HCT-116 (colon), HepG2 (hepatoma), A549 (lung) and U87 (glioma) as well as one normal cell line of HUVEC (human umbilical vein endothelial cells). Compounds **1–3** and NBDHEX were used as the positive controls. After 72 h treatment, the corresponding $IC_{50}$ values were obtained and given in Table 1. As shown in Table 1, compounds **1–3** exhibited insignificant cytotoxicity against the tested cancer cell lines, whereas the mixtrue of NBDHEX/**1** showed higher cytotoxicity than NBDHEX against the tested cancer cell lines. Interestingly, compounds **4** and **5**, consisting of NBDHEX and TDO inhibitor, possessed more potent cytotoxicity against all the tested cancer cell lines than the positive control with $IC_{50}$ values in the range of 1.36–4.33 μM and 1.98–5.50 μM, respectively. Synchronously **4** and **5** displayed lower cytotoxicity against HUVEC (35.45 and 37.18 μM, respectively) compared to NBDHEX and the mixture of NBDHEX /**1** (18.06 and 14.15 μM, respectively). Especially, compound **4** (a linker of succinic) displayed better anticancer activity than **5** (a linker of glutarate) against all the tested cancer cell lines. Additionally, as for HepG2, compounds **4** and **5** exhibited best anticancer activity with $IC_{50}$ values of 1.36 and 1.98 μM among the tested cancer cell lines. The superior antiproliferative activity of the conjugates may be due to their inhibition of tryptophan degradation [26b] and/or the better cellular uptake of the conjugates than the single or mixed drugs, which led to the more drug accumulation in tumor cells to kill cell. Based on the cytotoxicity assay, the level of TDO expression in the tested cancer cells were detected by western blot analysis. The results were showed in Fig. S7, all the tested cancer cell lines were determined to express TDO, especially, HepG2 cells owned the highest level of TDO protein. Hence, upon the above results, the following biological assays of **4** and **5** were focused on HepG2 cells.

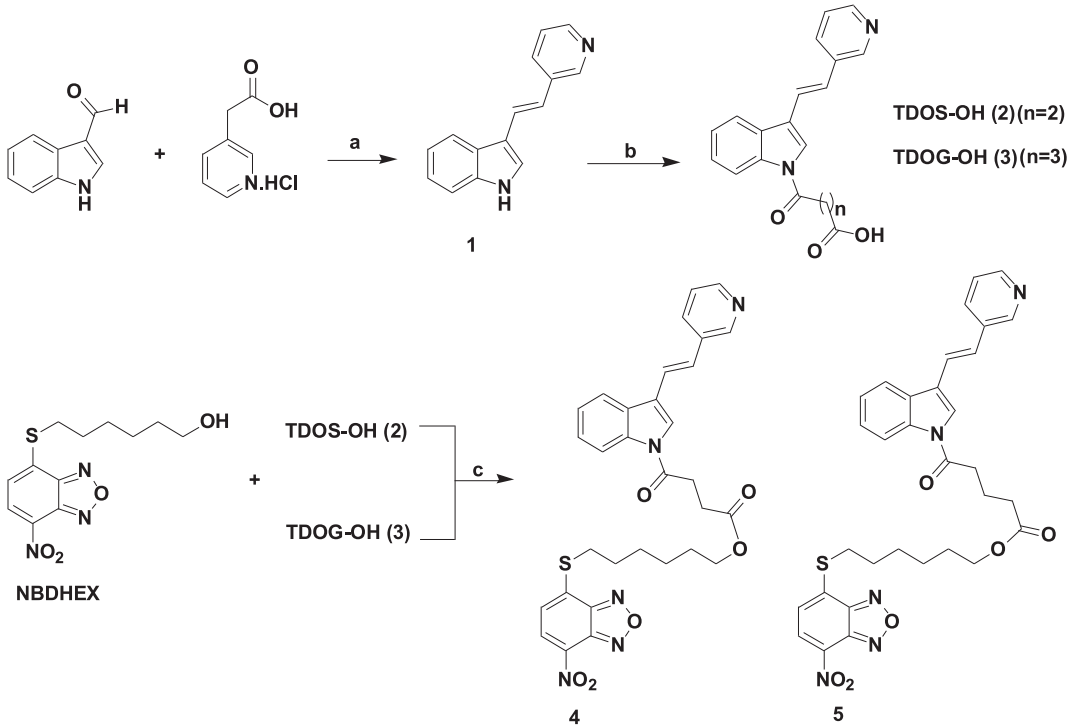


**Scheme 1.** Synthetic pathway to prepare target compounds **4** and **5**. Reagents and conditions: (a) dioxane, $Et_3N$, piperidine, 24 h; (b) succinic anhydride or glutaric anhydride, DMAP, $Et_3N$, $CH_2Cl_2$, 45 °C, 12 h; (c) EDCI, DMAP, DMF, room temperature, overnight.

**Table 1**
Cytotoxic effect of targeted compounds against different cancer cell lines.

| Compd | $IC_{50}$ (μM)[a] | | | | |
|---|---|---|---|---|---|
| | A549 | HCT-116 | U87 | HepG2 | HUVEC |
| NBDHEX | 10.99 ± 0.85 | 9.53 ± 0.82 | 8.45 ± 0.71 | 5.79 ± 0.24 | 18.06 ± 1.62 |
| NBDHEX:1 | 10.11 ± 0.82 | 8.31 ± 0.80 | 6.35 ± 0.60 | 4.40 ± 0.20 | 14.15 ± 1.29 |
| **1** | > 50 | > 50 | > 50 | > 50 | > 50 |
| **2** | > 50 | > 50 | > 50 | > 50 | > 50 |
| **3** | > 50 | > 50 | > 50 | > 50 | > 50 |
| **4** | 4.33 ± 0.37 | 3.08 ± 0.26 | 4.65 ± 0.38 | 1.36 ± 0.18 | 35.45 ± 0.71 |
| **5** | 5.01 ± 0.46 | 3.58 ± 0.27 | 5.50 ± 0.23 | 1.98 ± 0.09 | 37.18 ± 0.64 |

[a] $IC_{50}$ values are presented as the mean ± SD (standard error of the mean) from three independent experiments.

### 2.2.2. The inhibition of GSTs in HepG2 cells

Due to GSTs could catalyze the reaction of 1-chloro-2,4-dinitrobenzene (CDNB) with GSH to form GS-DNB adducts which could be detected at the absorption wavelength of 340 nm [38]. Hence, the activity of GSTs (extracted from HepG2 cells) following the treatment with the measured compounds were evaluated by spectrophotometer assay to detect the conjugation rate of 1-chloro-2,4-dinitrobenzene (CDNB) with GSH. As shown in Fig. 1, NBDHEX could efficiently inhibit the activity of GSTs at a dose-dependent manner. Satisfactorily, compounds **4** and **5** containing a TDO inhibitor with different linkers displayed more effective inhibitory ability than NBDHEX. These results indicated that the conjugates consisting of NBDHEX and TDO inhibitor by linkers could maintain the inhibitory activity of NBDHEX toward GSTs.

### 2.2.3. Compounds induced cell apoptotic

The mode of cell death induced by compounds **4** and **5** were investigated by FITC-Annexin V and propidium iodide (PI) double staining assay and the apoptotic rates of cancer cells were determined by flow cytometry. HepG2 cells were co-incubated with compounds **4** and **5** at 10 μM for 24 h with NBDHEX as a positive control. Q1, Q2, Q3, and Q4 represented: necrotic cells, late apoptotic or necrotic cells, early apoptotic cells and living cells, respectively. The results in Fig. 2 shown that compounds **4** and **5** exhibited high apoptotic rates of 71.4% and 66.5% (including late apoptotic and early apoptotic cells), respectively, which were obviously higher than NBDHEX (59.2%) and untreated group (5.34%). The results obviously indicated that the targeted compounds could effectively induce apoptosis, especially compound **4** was superior to **5.**

### 2.2.4. AO/EB staining

Acridine orange (AO) and ethidium bromide (EB), as vital dye, can stain cell nuclei with an intact cell membrane and the cells which lose their membrane integrity, respectively. To further confirm the apoptosis of HepG2 cells induced by the measured compounds, the AO/EB dual staining assay was carried out to evaluate the nuclear morphology of HepG2 cells. HepG2 cells were pretreated with the measured compounds at 10 μM for 24 h, and then stained with AO/EB and visualized under a fluorescence microscope. The live or dead cells are uniformly stained as green, while the apoptotic cells are thickly stained as red. As shown in Fig. 3, the green fluorescence was obviously decreased and concurrently the red fluorescence was markedly increased, which indicated that the apoptotic cells were increased and the live or dead cells were decreased after treatment with the measured compounds. And that both **4** and **5** showed higher apoptotic rates than NBDHEX. These results demonstrated that the target compounds could induce a strong amount of apoptotic effect in HepG2 cells.

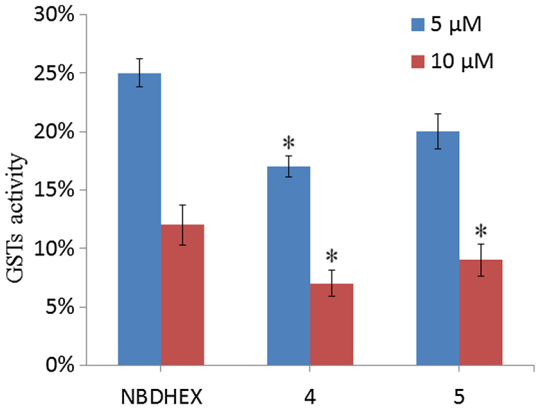


**Fig. 1.** The activity of GSTs after treatment with NBDHEX, compounds **4** and **5**. Mean values based on three independent experiments. (Mean ± SD, *P < 0.05, vs control group, ANOVA).

### 2.2.5. Effect on cell cycle arrest

To investigate the effect of compounds **4** and **5** on cell cycle arrest, we analyzed the cell cycle distributions of HepG2 cells by flow cytometry after 24 h treatment with the tested compounds at 10 μM, with NBDHEX as a positive control. It was noted from Fig. 4 that in the S phase, after treatment with NBDHEX at 10 μM, the percentage of S phase increased to 41.18% compared with the untreated group (25.33%). Interestingly, after treatments with **4** and **5,** the percentage of S phase was increased from 25.33% to 55.15% and 50.49%, respectively, as the percentage of cells in G1 phase decreased from 63.46% to 40.56% and 39.72%, respectively. These observations revealed that **4** and **5** mainly arrested the cell cycle at S phase.

### 2.2.6. Compounds induced apoptosis via the regulation of apoptosis related protein expression

The mitochondrial apoptotic pathway is a major signaling way to involve in tumor cells apoptosis via regulating associated protein [39]. To further investigate the mechanism of action of the newly synthesized compounds, the mitochondrial apoptotic pathway associated proteins of Bax, Bcl-2, caspase-3 and PARP in HepG2 cells were detected by western blot analysis. After HepG2 cells were treated with 10 μM of the tested compounds, the apoptosis-related proteins levels were determined and the results were showed in Fig. 5. After treatment with **4** and **5**, the Bcl-2 family including Bcl-2 (antiapoptotic protein) and Bax (pro-apoptotic protein) significantly changed, the level of Bcl-2 was significantly down-regulated, while the proapoptotic protein Bax was markedly up-regulated compared to the NBDHEX and untreated groups. In addition, the downstream protein of active-caspase 3 and cleavage-PARP were remarkably increased which could contribute to cell apoptosis. These observations suggested that compounds **4** and **5** might induce HepG2 cells apoptosis via a mitochondrial apoptotic pathway, especially the effect of **4** was superior to that of **5**.

### 2.2.7. The expression of TDO in HepG2 cells

The TDO enzyme overexpressed in tumor can cause

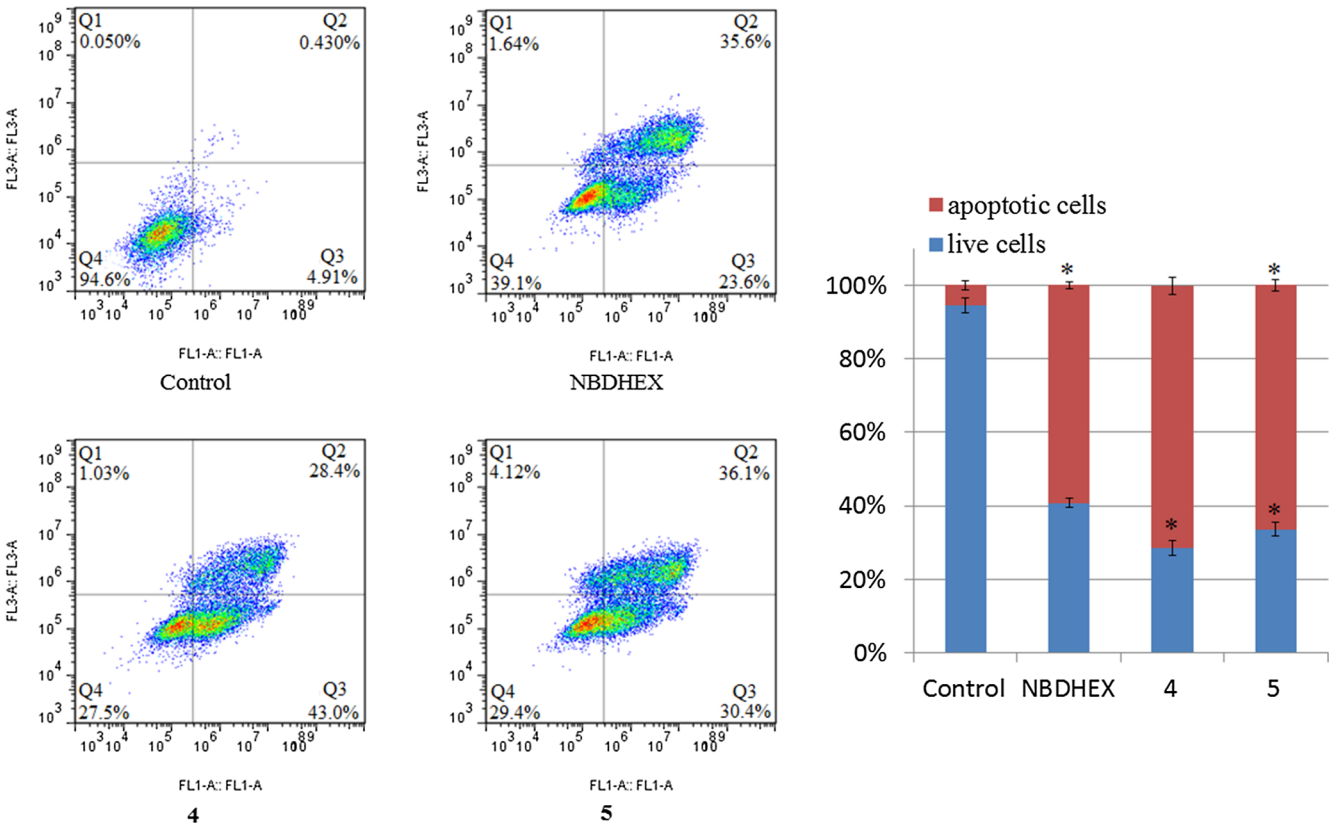


**Fig. 2.** Annexin V-FITC and PI double staining to evaluate HepG2 cells apoptosis after treatment with the measured compounds. HepG2 cells were treated with compounds (10 μM) for 24 h, incubated with Annexin V-FITC and PI and analyzed using flow cytometry. Data represent three independent experiments. (Mean ± SD, *P < 0.05, vs control group, ANOVA).

immunosuppression, hence the blockade of TDO protein expression can reverse T cell dysfunction and exhaustion to enhance antitumor immunity [31]. Herein, we investigated the TDO activity and protein expression inhibitory potency by **4** and **5** in HepG2 cells via western blotting and qRT-PCR analyses with **1** and NBDHEX as positive control. As shown in Fig. 6A, compounds **1**, **4** and **5** could effective inhibit TDO protein expression in contrast to the control group, but NBDHEX displayed insignificant inhibition. Intriguingly, **4** showed the most markedly efficacy to inhibit the expression of TDO protein (including higher inhibitory effect than **1**), particularly in a time-dependent manner (Fig. 6B). In addition, the qRT-PCR analyses revealed that compound **4** could down-regulate the level of TDO mRNA expression in a time-dependent manner after treatment with **4** (10 μM) for 24, 48 and 72 h, respectively (Fig. 6C). All of these results indicated that the targeted compounds could effectively inhibit the expression of TDO protein, especially compound **4** was optimal.

### 2.2.8. Cell-based kynurenine inhibition assay

Many studies suggested that inhibition of TDO protein expression can block tryptophan to be catabolized to produce kynurenine, which leads to the improvement of system immunity to enhance the efficacy of cancer treatments [27–31]. Hence, we examined the level of kynurenine production in HepG2 cells by HPLC after treatment with compound **4** (10 μM) for 24 h. The result was showed in Fig. 7A, compound **4**, had a stronger effect to inhibit the expression of TDO, also obviously down-regulated the level of kynurenine production compared to the control group and compound **1**. The result confirmed that **4** could reduce the level of kynurenine production via blocking TDO protein expression.

### 2.2.9. (q)RT-PCR of AHR mRNA expression level in HepG2 cells

It was reported that the Kyn-mediated activation of aryl hydrocarbon receptor (AHR) could promote cancer cells survival and involve in the regulation of anticancer immunity [32,40]. Compound **4** could block TDO expression to inhibit kynurenine, which may lead to inactivation of AHR. Hence, to support this hypothesis, the mRNA expression level of AHR in HepG2 cells was detected by qPCR analyses. After HepG2 cells were treated with **4** at 10 μM for the appointed times, the RNA in HepG2 cells was harvested for qPCR. As shown in Fig. 7B, the mRNA expression levels of AHR were markedly decreased in a time-dependent manner compared to the untreated group. This result support that **4** could inactivate the downstream of AHR, thereby destabilizing TDO-AHR pathway.

### 2.2.10. Evaluation of T-cell immune responses

To investigate the immunomodulatory capacity of compound **4**, a mixed leukocyte reaction (MLR) was carried out to examine the cellular immune response. Here, peripheral blood mononuclear cells (PBMCs), which from unrelated healthy donors, co-cultured with HepG2 cells after stimulated with a lectin of phytohemagglutinin and stained with carboxyfluorescein succinimidyl ester (CFSE). After treated with the measured compounds, the PBMCs were harvested and stained with anti-$CD3^+$ antibodies ($CD3^+$ is a marker representing the development of *T*-cell). Then the proliferation of $CD3^+$ *T*-cell were analyzed by flow cytometry. As shown in Fig. 8, all the tested compounds (10 μM) can effectively stimulate $CD3^+$ *T*-cell proliferation. Significantly, HepG2/MLR co-cultured with compound **4** (proliferative rate of 54.54%) was the most effective system in stimulating $CD3^+$ *T*-cell proliferation compared to the other groups. These results demonstrated that compound **4** might improve antitumor immune response by stimulating $CD3^+$ *T*-cell activation and proliferation.

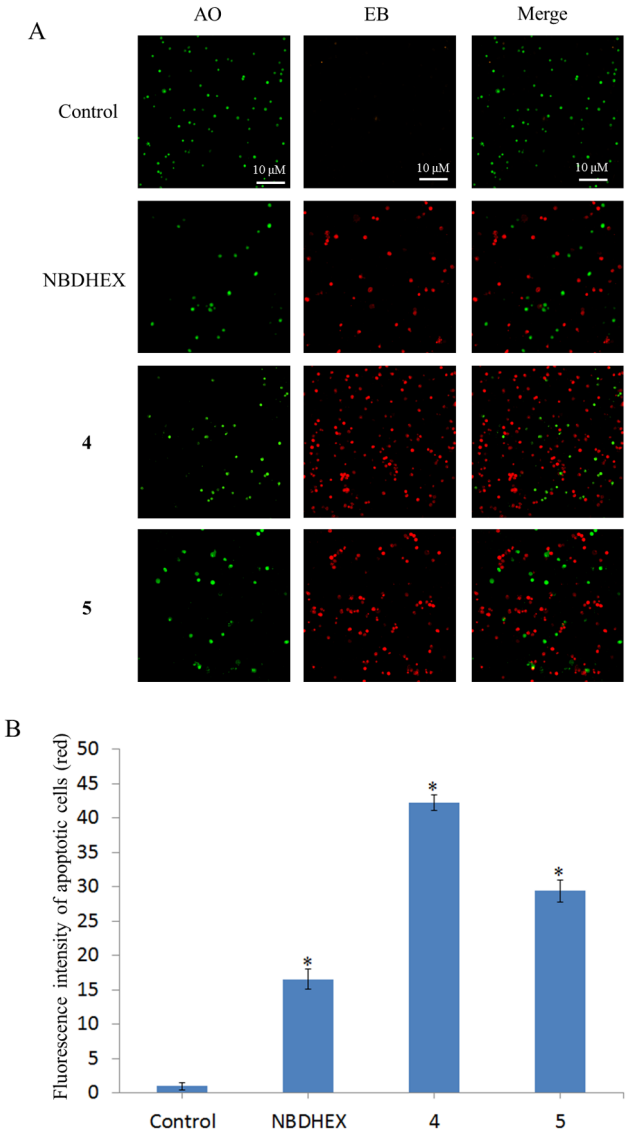


**Fig. 3.** (A) AO/EB staining of compounds NBDHEX, **4** and **5** in HepG2 cells at 10 μM for 24 h with an untreated group as control. (B) Mean fluorescence intensity of apoptotic cells (red). The apoptotic cells (red) and live cells (green) after treatment with compounds for 24 h (10 × magnification). Data represent three independent experiments. (Mean ± SD, *P < 0.05, vs control group, ANOVA).

## 3. Conclusions

In conclusion, we present a strategy of checkpoint inhibitor platform that dual suppression of the immunosuppressive enzyme TDO and glutathione S-transferase to enhance antitumor immune response. The cytotoxicity assays showed that the two novel conjugates displayed significantly antitumor activity against HepG2 cancer cells and low toxicity against normal human cell line (HUVEC) *in vitro*. Further mechanistic evaluations revealed that compound **4** could inhibit GSTs expression, increase the G1 population and induce apoptosis in cancer cells via a mitochondrial-dependent apoptosis pathway. Interestingly, **4** displayed more effectively inhibition of TDO protein expression than **5** and led to the decrease of Kyn production and the deactivation of AHR, which may improve immune response via boosting $CD3^+$ *T*-cell activation and proliferation. Consequently, such an immuno-chemotherapeutic strategy via combining TDO and GSTs inhibitors may regulate antitumor immune response by inhibiting TDO and GSTs. This rational design offers a potential strategy for HCC treatment.

## 4. Experimental section

### 4.1. Chemistry

All the analytical grade of chemical reagents and solvents were acquired from commercial resources and used without further purification, unless noted specifically. All cancer cell lines included cancer and normal were purchased from Nanjing KeyGEN BioTECH Company (China). $^1$H NMR and $^{13}$CNMR were recorded on a BRUKER AV-400/600 spectrometer in $CDCl_3$ or DMSO-$d_6$ with TMS as an internal standard. Mass spectra were measured with an Agilent 6224 TOF LC/MS instrument. Cell cycle and apoptosis assay were carried out by using flow cytometry (FAC Scan, Becton Dickenson). Human peripheral blood mononuclear cells (PBMCs) were from unrelated healthy donors of blood (approved by donors themselves), all procedures were performed in compliance with relevant laws and institutional guidelines. CFSE-conjugated anti-$CD3^+$ antibody (Abcam) and anti-TDO2 (Abcam) were purchased for flow cytometry and western bloting. The β-acitn, Bax, Bcl-2, caspase-3, PAPR antibodies were purchased from Imgenex, USA.

#### 4.1.1. Synthesis of compound *1*

Compound **1** was prepared according to the method of a literature reported [28]. The pyrid-3-ylacetic acid hydrochloride (0.9 g, 5.2 mM) and triethylamine (1.4 g, 13.1 mM) were dissolved in dioxane (15 mL), and the mixture was stirred at room temperature for about 10 min. Then 1H-indole-3-carbaldehyde (0.5 g, 3.5 mM) and piperidine (0.6 g, 15.2 mM) were added, and the resulting mixture was stirred at reflux temperature for one day. After the reaction was completed, the solution was diluted with ethyl acetate, evaporated with silica and purified by flash chromatography to give the product. Yield: 1.06 g (83%). $^1$H NMR (400 MHz, DMSO-$d_6$) $\delta$ 11.42 (s, 1H), 8.77 (d, $J$ = 2.1 Hz, 1H), 8.38 (dd, $J$ = 4.7, 1.5 Hz, 1H), 8.06 (d, $J$ = 7.8 Hz, 1H), 8.02 (dt, $J$ = 8.0, 1.9 Hz, 1H), 7.69 (d, $J$ = 2.6 Hz, 1H), 7.57 (d, $J$ = 16.6 Hz, 1H), 7.45 (d, $J$ = 8.0 Hz, 1H), 7.36 (dd, $J$ = 7.9, 4.7 Hz, 1H), 7.21–7.17 (m, 1H), 7.16–7.10 (m, 2H). HRMS (ESI) *m/z* calculated for $C_{15}H_{12}N_2$ $[M+H]^+$: 221.10375, found: 221.10375.

#### 4.1.2. Synthesis of compound *2*

A mixture of **1** (0.5 g, 2.3 mM), succinic anhydride (0.4 g, 3.5 mM), DMAP (28 mg, 0.23 mM) and $CH_2Cl_2$ (40 mL) was charged in a 100 mL flask, then triethylamine (0.7 g, 6.9 mM) was added at room temperature. The resulting solution was heated to 45 °C and then maintained at 45 °C for 24 h. Upon completion of the reaction, the mixture was concentrated to remove the solvent and the title compound was obtained by flash chromatography to give **2** as a pale yellow solid (0.6 g, 73%). $^1$H NMR (400 MHz, DMSO-$d_6$) $\delta$ 12.27 (s, 1H), 8.83 (d, $J$ = 2.1 Hz, 1H), 8.46 (dd, $J$ = 4.7, 1.5 Hz, 1H), 8.40 (dd, $J$ = 7.2, 1.4 Hz, 1H), 8.32 (s, 1H), 8.13 (dd, $J$ = 6.8, 1.6 Hz, 1H), 8.10 (dt, $J$ = 7.9, 1.8 Hz, 1H), 7.58 (d, $J$ = 16.7 Hz, 1H), 7.44–7.37 (m, 4H), 3.32 (d, $J$ = 6.8 Hz, 2H), 2.73–2.68 (m, 2H). HRMS (ESI) *m/z* calculated for $C_{19}H_{16}N_2O_3$ $[M+H]^+$: 321.12104, found: 321.12104.

#### 4.1.3. Synthesis of compound *3*

Similar to the preparation of **2**, glutaric anhydride instead of succinic anhydride was used to carry out the reaction to give compound **3** as a pale yellow solid (0.7 g, 78%). $^1$H NMR (400 MHz, DMSO-$d_6$)$\delta$ 12.15 (s, 1H), 8.82 (d, $J$ = 2.0 Hz, 1H), 8.46 (dd, $J$ = 4.7, 1.3 Hz, 1H), 8.43 (d, $J$ = 7.9 Hz, 1H), 8.25 (s, 1H), 8.12 (d, $J$ = 7.5 Hz, 1H), 8.09 (d, $J$ = 8.0 Hz, 1H), 7.57 (d, $J$ = 16.7 Hz, 1H), 7.45–7.42 (m, 1H), 7.42–7.39 (m, 2H), 7.38–7.36 (m, 1H), 3.13 (t, $J$ = 7.3 Hz, 2H), 2.41 (t, $J$ = 7.3 Hz, 2H), 1.96 (p, $J$ = 7.3 Hz, 2H). HRMS (ESI) *m/z* calculated for $C_{20}H_{18}N_2O_3$ $[M+H]^+$: 335.14297, found: 335.14297.

#### 4.1.4. Synthesis of NBDHEX

The compound of NBDHEX was prepared following the reported protocols [16]. NBD-Cl (0.50 mg, 2.5 mM) and 6-mercapto-1-hexanol

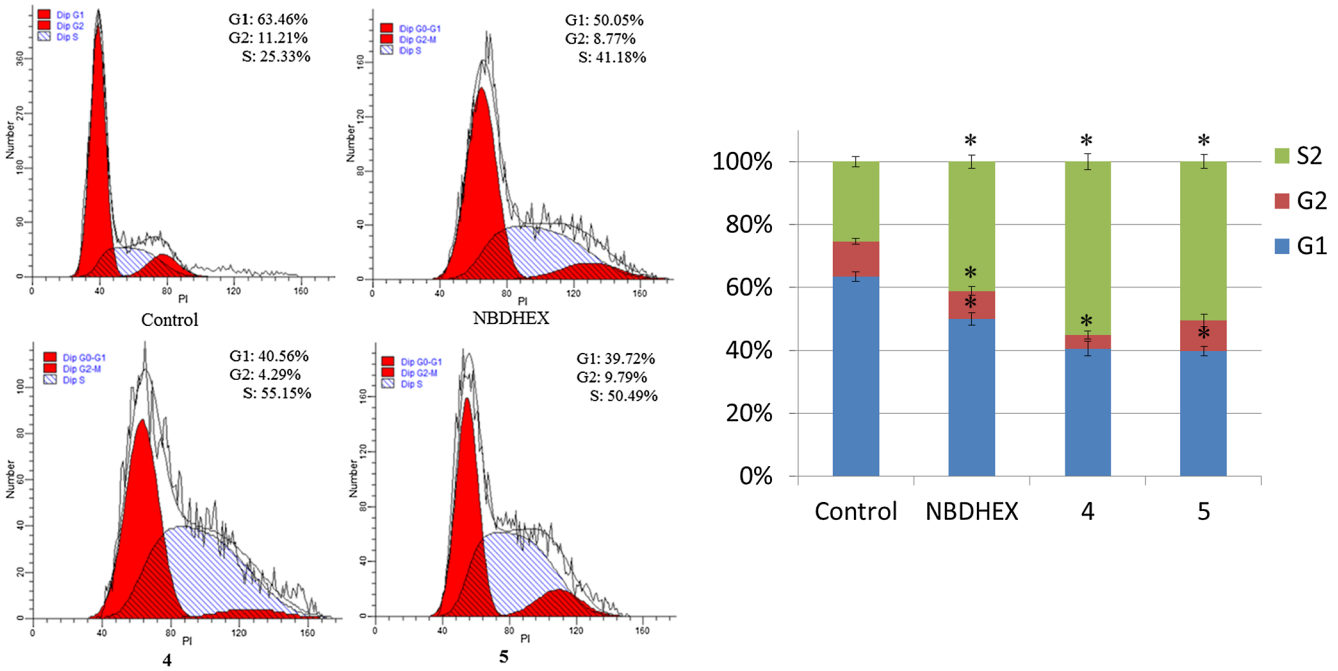


**Fig. 4.** Compounds induced cell cycle arrest at S phase. HepG2 cells were pretreated with 10 μM compounds for 24 h. Then cells were fixed, stained with propidium iodide (PI), and assessed by flow cytometry. The untreated cells were used for comparison. The experiments were performed three times, and the results of the representative experiments are shown. (Mean ± SD, *P < 0.05, vs control group, ANOVA).

(0.67 mg, 5 mM) were dissolved in 40 mL of a 1:1 (v/v) mixture of ethanol and 0.1 M potassium phosphate buffer in a closed vessel, and stirred at 25 °C for 6 h. The pH was adjusted by suitable addition of 1 M KOH to keep neutral. Upon completion of the reaction, the excess of 6-mercapto-1-hexanol was removed by adding 1.5 mM of 3-bromopyruvate. The target product of NBDHEX (dark yellow) was collected by filtration and washed with cold distilled water (2 × 15 mL). $^1$H NMR (600 MHz, $CDCl_3$) $\delta$ 8.40 (d, $J$ = 7.9 Hz, 1H), 7.14 (d, $J$ = 7.9 Hz, 1H), 3.67 (t, $J$ = 6.4 Hz, 2H), 3.27 (t, $J$ = 7.4 Hz, 2H), 1.87 (dt, $J$ = 15.1, 7.4 Hz, 2H), 1.61–1.56 (m, 4H), 1.49–1.44 (m, 2H), 1.24 (s, 1H).

### 4.1.5. Synthesis of compound 4

Compound **2** (100 mg, 0.31 mM), TBTU (150 mg, 0.47 mM) and triethylamine (48 mg, 0.47 mM) were dissolved in dried DMF (10 mL) and stirred for 10 min, then NBDHEX (100 mg, 0.33 mM) was added to the mixture. The resulting solution was stirred at room temperature for overnight. After completion, the solution was diluted with $CH_2Cl_2$ (120 mL) and washed with water (3 × 150 mL), dried over with anhydrous $Na_2SO_4$. The crude product was purified by column chromatograph using petroleum ether/ethyl acetate (2:1 v/v) as the eluent to give a dark yellow solid (145 mg, 73.2%). $^1$H NMR (600 MHz, DMSO-$d_6$) $\delta$ 8.83 (d, $J$ = 4.4 Hz, 1H), 8.52–8.43 (m, 2H), 8.33 (d, $J$ = 6.8 Hz, 1H), 8.27 (d, $J$ = 6.3 Hz, 1H), 8.19 (s, 1H), 8.05 (s, 1H), 7.59–7.50 (m, 2H), 7.40–7.30 (m, 4H), 4.06 (d, $J$ = 5.9 Hz, 2H), 3.36 (d, $J$ = 4.4 Hz, 2H), 3.20 (d, $J$ = 6.6 Hz, 2H), 2.77 (d, $J$ = 4.5 Hz, 2H), 1.63 (d, $J$ = 6.2 Hz, 2H), 1.56 (d, $J$ = 5.9 Hz, 2H), 1.39 (s, 2H), 1.32 (s, 2H). $^{13}$C NMR (150 MHz, DMSO) $\delta$ 172.57, 171.37, 149.42, 146.92, 146.75, 142.94, 140.56, 136.13, 134.44, 134.36, 132.64, 132.29, 128.42, 125.82, 125.65, 124.89, 124.82, 124.37, 122.96, 122.23, 120.67, 119.53, 116.48, 64.36, 30.87, 30.79, 28.78, 28.43, 28.25, 27.67, 25.26. HRMS (ESI) $m/z$ calculated for $C_{31}H_{29}N_5O_6S$ $[M+H]^+$: 600.19833, found: 600.19833.

### 4.1.6. Synthesis of compound 5

Prepared **5** according to the procedure described for compound **4**. NBDHEX was stirred with **3**, and then purified on silica to give compound **5** as a dark yellow solid (152 mg, 76.4%). $^1$H NMR (600 MHz, $CDCl_3$) $\delta$ 8.74 (s, 1H), 8.48 (d, $J$ = 20.0 Hz, 2H), 8.32 (t, $J$ = 6.5 Hz, 1H), 7.85 (d, $J$ = 6.5 Hz, 2H), 7.66 (d, $J$ = 4.5 Hz, 1H), 7.41–7.31 (m, 3H), 7.27–7.21 (m, 1H), 7.15 (dd, $J$ = 16.5, 5.1 Hz, 1H), 7.09–7.03 (m,

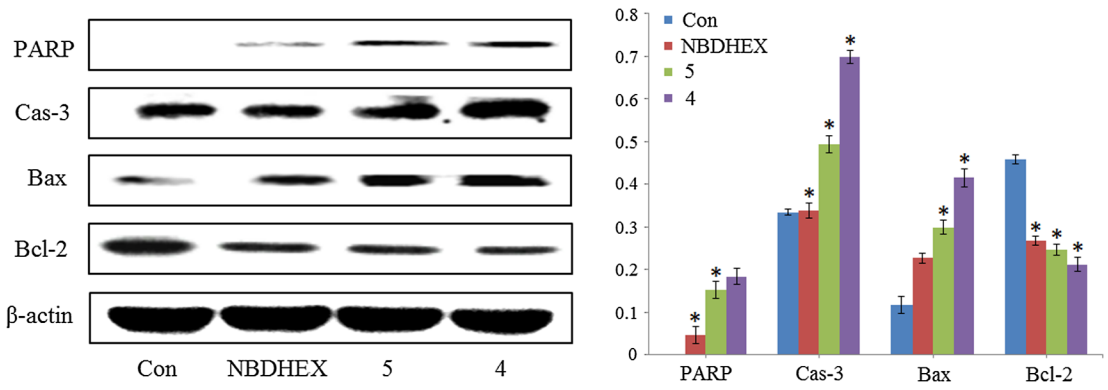


**Fig. 5.** Western blotting analysis of the expression of related proteins after treatment with the tested compounds at 10 μM for 24 h. (Mean ± SD, *P < 0.05, vs control group, ANOVA).

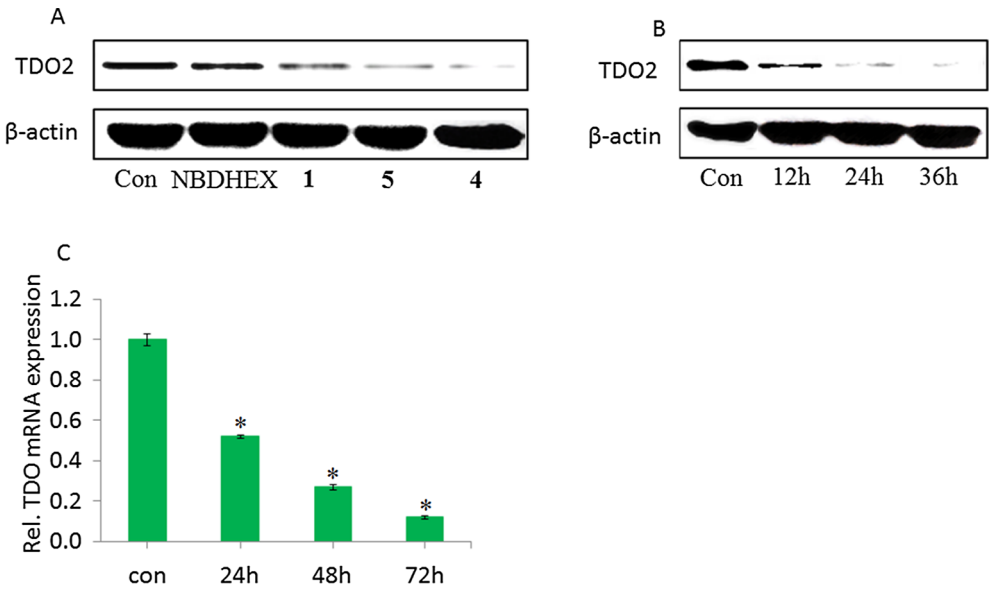


**Fig. 6.** (A) Western blotting of TDO expression level in HepG2 cells after treatment with the tested compounds at 10 μM for 24 h. (B) Western blotting of the time-dependent (12, 24, 36 h) inhibition of TDO expression by **4** in HepG2 cells. (C) qRT-PCR of time-dependent (24, 48, 72 h) TDO mRNA after treatment with **4** (10 μM). Data represent three individual experiments (Mean ± SD, *P < 0.05, vs control group, ANOVA).

1H), 4.12 (d, $J$ = 5.4 Hz, 2H), 3.22 (d, $J$ = 5.9 Hz, 2H), 3.04 (d, $J$ = 5.7 Hz, 2H), 2.54 (d, $J$ = 5.5 Hz, 2H), 2.18 (d, $J$ = 5.9 Hz, 2H), 1.83 (d, $J$ = 6.1 Hz, 2H), 1.68 (d, $J$ = 5.9 Hz, 2H), 1.55 (d, $J$ = 5.6 Hz, 2H), 1.44 (d, $J$ = 5.3 Hz, 2H). $^{13}$C NMR (150 MHz, $CDCl_3$) $\delta$ 173.15, 170.54, 149.13, 148.06, 147.76, 142.43, 141.83, 136.44, 133.35, 132.79, 132.37, 130.74, 128.24, 125.88, 125.58, 124.19, 123.84, 123.27, 121.92, 120.22, 120.12, 119.84, 116.88, 64.39, 34.78, 33.02, 31.64, 28.48, 28.39, 27.71, 25.53, 19.73. HRMS (ESI) *m/z* calculated for $C_{32}H_{31}N_5O_6S$ $[M+H]^+$: 614.21099, found: 614.21099.

### 4.2. Biology

#### 4.2.1. Cytotoxicity analysis

*Cell culture*. HepG2 (human hepatoma cancer cell line), A549 (human lung cancer cell line), HCT-116 (human colorectal cell line), U87 (Human glioma cell line), and HUVEC (normal human umbilical vein endothelial cell line) were purchased from Nanjing KeyGEN BioTECH Company (China). The cells were maintained in DMEM medium containing 10% fetal bovine serum, 100 mg/mL of penicillin and 100 mg/mL of streptomycin at 37 °C in a 5% carbon dioxide atmosphere.

*MTT assay*. All tested compounds were prepared as 2 mM solution in DMSO and diluted in culture medium at six different concentrations. The *in vitro* cytotoxicity of the tested compounds was determined by the MTT assay. Briefly, about 5 × $10^4$ cells/mLin DMEM medium with 10% FBS in each well of 96-well plates and incubated overnight at 37 °C in 5% $CO_2$. The various concentrations of compounds were added to the test well, then incubated at 37 °C (5% $CO_2$ atmosphere). After 72 h, the medium in each well was replaced by the serum-free medium containing 1 mg/mL MTT and incubated for an additional 4 h. The medium was removed and subsequently 100 μL of DMSO was added. The UV absorption intensity was detected with an ELISA reader at 490 nm. Cytotoxicity was determined on the percentage of cell survival compared with the negative control. The $IC_{50}$ values were calculated by the Bliss method, the reported $IC_{50}$ values are the average at least three independent experiments.

#### 4.2.2. GSTs activity

The activity of GSTs was analyzed at 340 nm by spectrophotometer assay to measure the conjugation rate of CDNB with GSH as a function of time according to the reported previously [38]. Briefly, GSTs were extracted from HepG2 cells and the tested compounds were added to 0.1 M potassium phosphate buffer (pH 6.5), and the mixture was incubated at room temperature for 5 min. Then CDNB and GSH were added and quickly mixed well. Absorbance was measured at 340 nm for 5 min at 20 °C. Before each experiment, the baseline of the UV spectrometer was corrected by replacing GST solution with phosphate buffer. All of the tests were repeated in triplicate.

#### 4.2.3. AO/EB staining

The AO/EB dual staining was carried out to evaluate the live and apoptotic cells. The tested compounds were prepared in DMSO at the

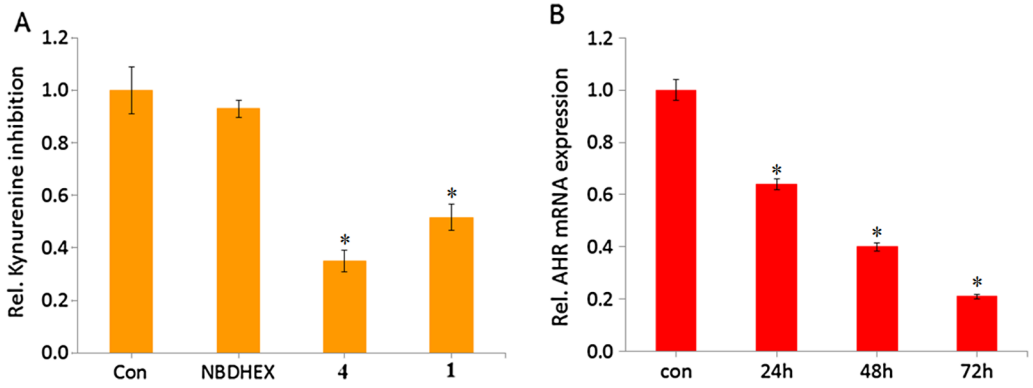


**Fig. 7.** (A) The inhibition of kynurenine after treatment of HepG2 cells with **4** (10 μM) in comparison to **1** and an untreated control. (B) qRT-PCR of AHR mRNA after treatment with **4** (10 μM) for 24 h, 48 h and 72 h. Data represent three individual experiments (Mean ± SD, *P < 0.05, vs control group, ANOVA).

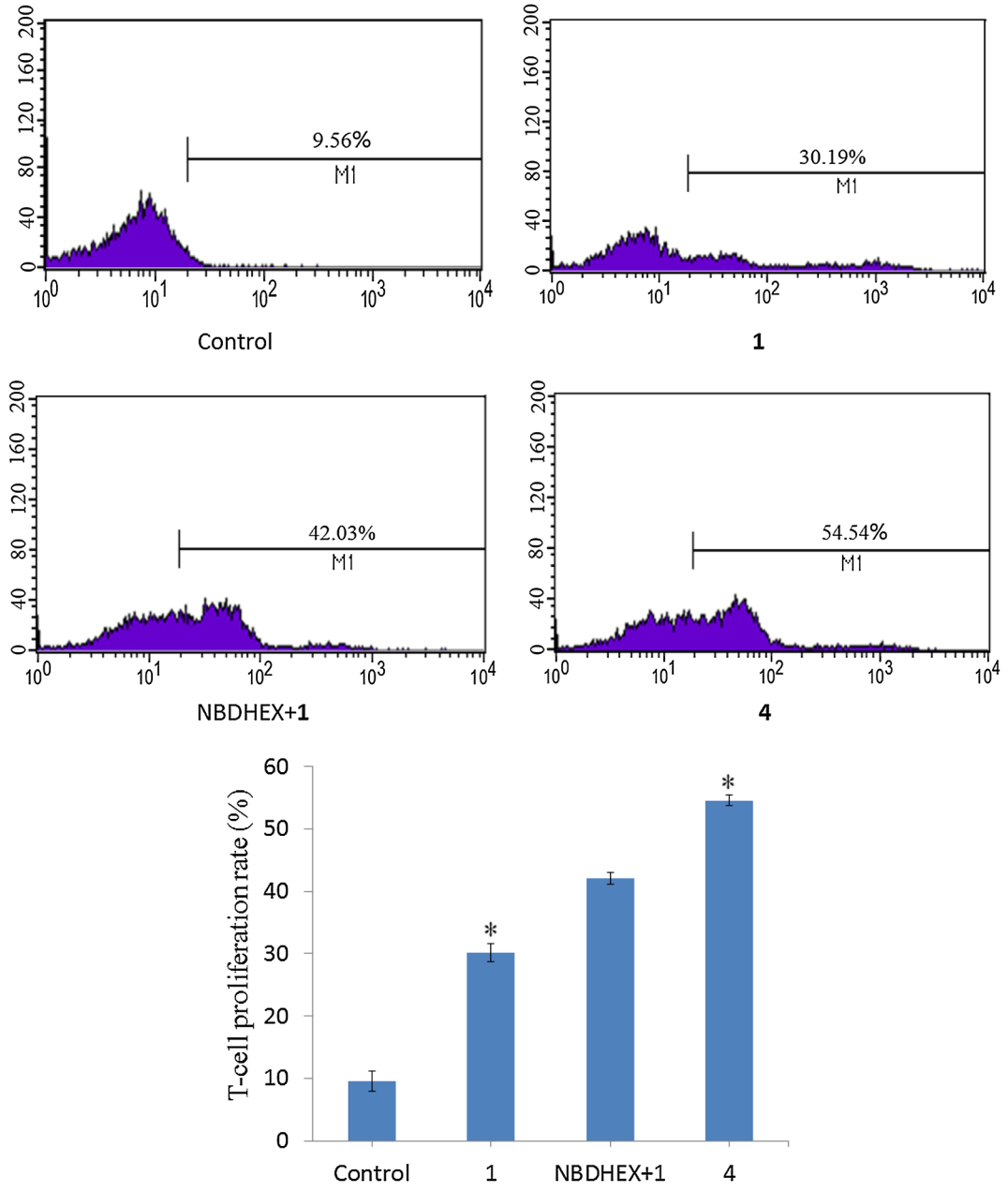


**Fig. 8.** Mixed leukocyte reaction to evaluate $CD3^+$ *T*-cell proliferation after compounds (10 μM) incubated with PBMCs and HepG2 cells for 6 days. Data represent three individual experiments (Mean ± SD, *P < 0.05, vs control group, ANOVA).

indicated concentration. HepG2 cells were seeded into 6-well plates in 10% FBS-DMEM and cultured overnight in 5% $CO_2$ at 37 °C. Then, the medium was removed and added into fresh medium plus 10% fetal bovine serum and treated with 10 μM of the tested compounds. After treatment for 24 h, the cells were harvested, suspended in PBS, then the cover slip with monolayer cells was inverted on a glass slide with 20 mL of AO/EB stain. Fluorescence was read on an Nikon ECLIPSETE2000-S fluorescence microscope (OLYMPUS Co., Japan).

*4.2.4. Apoptosis analysis*

The flow cytometry analysis of Annexin V and PI staining assay was performed to evaluate apoptotic rates. HepG2 cells were seeded into 6-well plates at the density of $2 \times 10^6$/well in 10% FBS-DMEM to the final volume of 2 mL. After cultured overnight, the tested compounds (10 μM) were added and incubated for 24 h. The cells were digested with trypsin and washed twice with cold PBS, then collected and re-suspended cells in binding buffer at a concentration of $1 \times 10^6$ cells/mL. To 100 μL of the solution in a 5 mL culture tube, 5 mL of FITC Annexin V (BD, Pharmingen) and 5 mL propidium iodide (PI) were added, then annexin-V FITC apoptosis kit was used. The cells were gently vortexed and incubated for 30 min at room temperature in the dark. The apoptotic experiment was analyzed using the system software (Cell Quest; BD Biosciences).

*4.2.5. Cell cycle measurement*

HepG2 cells were seeded in 6-well plates and cultured overnight at 37 °C in 5% $CO_2$, and then treated with 10 μM of the tested compounds. After co-incubated for 24 h, cells were collected with centrifugation and washed twice with ice-cold PBS. The cell pellets were resuspended and fixed with ice-cold 70% ethanol at 4 °C overnight. The cells were washed with ice-cold PBS and pretreated with 100 μg/mL RNase at 37 °C for 30 min, and finally stained with 50 μg/mL propidium iodide (PI) in the dark at 4 °C for 30 min. Cell cycle was measured by flow cytometry (FAC Scan, Becton Dickenson) using Cell Quest software and recording

propidium iodide (PI) in the FL2 channel.

#### 4.2.6. Western blotting analysis

The HepG2 cells ($1 \times 10^6$) were cultured with 10 μM of the tested compounds for 24 h at 37 °C. After for 24 h, cells were collected and washed twice with ice-cold PBS. And then the cells were lysed in cell lysis buffer containing PMSF for 30 min, lysates were centrifugated and collected at 4 °C for 10 min. The concentration of protein was measured by the BCA (bicinchoninic acid) protein assay reagents. Equal amounts of protein per line was separated on 12% SDS polyacrylamide gel electrophoresis and transferred to PVDF Hybond-P membrane (GE Healthcare). Membranes were incubated with 5% skim milk in Tris-buffered saline with Tween 20 (TBST) buffer for 1 h and then the membranes being gently rotated overnight at 4 °C. Membranes were incubated with primary antibodies at 4 °C overnight. Next, membranes incubated with peroxidase labeled secondary antibodies for 2 h at 25 °C. The protein blots were detected by chemiluminescence reagent (Thermo Fischer Scientifics Ltd.). β-actin was used as the loading control.

#### 4.2.7. The level of kynurenine determined by HPLC

The level of kynurenine was detected according to literature method [26]. HepG2 cells ($2 \times 10^5$ cells) were seeded in a 6-well plate with 2 mL medium (containing 10% FBS, 100 U/mL penicillin, and 100 μg/mL streptomycin). Next day, the medium was removed and replaced with fresh medium, then the tested compounds were added. After 48 h of incubation, the cells were collected by centrifugation, and mixed with the 100 μL 20% trichloroacetic acid for protein precipitation. After incubated for 30 min at 50°C, the sample was centrifuged for 10 min at 3000*g* to remove the sediments, and the supernatant was analyzed by HPLC. Reversed phase HPLC was implemented on a 250 × 4.5 mm ODS column and the HPLC profiles were recorded on UV detection at 360 nm. Mobile phase consisted of acetonitrile/water, and flow rate was 1 mL/min. The samples were taken for HPLC analysis after filtration by 0.45 μm filter.

#### 4.2.8. Quantitative (q)RT-PCR

The mRNA levels of TDO and AHR were detected by qRT-PCR assay as described previously [26]. After incubated with the targeted compounds, HepG2 cells were collected to obtain the RNA for further analysis. Total RNA isolated with the Qiagen RNAeasy kitand cDNA was synthesized with the Applied Biosystems reverse-transcription-kit. (q) RT-PCR was performed in a Lightcycler 480 II thermo cycler with SYBR Green PCR Mastermix (Roche). All primers were separated by at least one intron on the genomic DNA to exclude its amplification. PCR reactions were checked by including no-RT controls, by omission of templates, and melting curves. Standard curves were generated for each gene. Relative quantification of gene expression was determined by comparison of threshold values. All samples were analyzed in duplicate at two different dilutions. All results were normalized to GAPDH.

Primer sequences were (5′-3′ forward, reverse):
TGTTGCCATCAATGACCCCTT; CTCCACGACGTACTCAGCG (GAPDH)
GGCCGTGTCGATGTATCAGT; GCCTGGCAGTACTGGATTGT (AHR)
CGGTGGTTCCTCAGGCTATC; CTTCGGTATCCAGTGTCGGG (TDO)

#### 4.2.9. T-cell proliferation analysis

A mixed leukocyte reaction (MLR) assay was performed to evaluate T cells proliferation as described previously [26]. HepG2 cells were seeded in 6-well plates ($1 \times 10^5$ cells/well). After cultivation for 24 h, the cells were replaced with fresh DMEM and treated with indicated concentrations of compounds. The HepG2 cells were incubated with different compounds for 2 d at 37 °C. PBMCs ($2 \times 10^5$ cells/well) stained with CellTraceTM Far Red Cell Proliferation Kit (CFSE) were subsequently inserted after PHA-M stimulation. After co-cultured for 6 days at 37 °C, the PBMCs were centrifuged and collected for further analysis. The cell pellets were resuspended in PBS and stained with FITC-conjugated anti-CD3 antibody. The *T*-cell proliferation was measured by flow cytometry.

### 4.3. Statistical analysis

All experiments were replicated three independent experiments and data was presented as mean ± SD. Differences between groups were assessed using one-way ANOVA. $P < 0.05$ was set as the criterion of statistical significance.

## Declaration of Competing Interest

The authors declare no competing financial interest.

## Acknowledgments

We are grateful to the National Natural Science Foundation of China (Grant Nos. 21571033 and 81503099) for financial aids to this work. The authors would also like to thank the Fundamental Research Funds for the Central Universities (Project 2242017K41024) and Zhishan Youth Scholar Program of SEU (2242019R40045) for supplying basic facilities to our key laboratory.

## Appendix A. Supplementary material

Supplementary data to this article can be found online at https://doi.org/10.1016/j.bioorg.2019.103191.

## References

[1] L.K. Kheyrabadi, M.A. Mehrgardi, E. Wiechec, A.P.F. Turner, A. Tiwari, Ultrasensitive detection of human liver hepatocellular carcinoma cells using a label-free aptasensor, Anal. Chem. 86 (2014) 4956–4960.
[2] F. Bray, J. Ferlay, I. Soerjomataram, R.L. Siegel, L.A. Torre, A. Jemal, Global cancer statistics 2018: GLOBOCAN estimates of incidence and mortality worldwide for 36 cancers in 185 countries, Ca. Cancer. J. Clin. 68 (2018) 394–424.
[3] K.J. Lafaro, A.N. Demirjian, T.M. Pawlik, Epidemiology of hepatocellular carcinoma, Surg. Oncol. Clin. N. Am. 24 (2015) 1–17.
[4] J. Xie, A.H. Zhang, X.J. Wang, Metabolomic applications in hepatocellular carcinoma: toward the exploration of therapeutics and diagnosis through small molecules, RSC. Adv. 7 (2017) 17217–17226.
[5] R. JulieH, G. YezazAhmed, M. Idrees, Review of hepatocellular carcinoma: Epidemiology, etiology, and carcinogenesis, J. Carcinog. 16 (2017) 1–11.
[6] L. Beretta, Comparative analysis of the liver and plasma proteomes as a novel and powerful strategy for hepatocellular carcinoma biomarker discovery, Cancer Lett. 286 (2009) 134–139.
[7] Y.Y. Lee, K.Q. McKinney, S. Ghosh, D.A. Iannitti, J.B. Martinie, F.R. Caballes, M.W. Russo, W.A. Ahrens, D.H. Lundgren, D.K. Han, H.L. Bonkovsky, S. Hwang, Subcellular tissue proteomics of hepatocellular carcinoma for molecular signature discovery, J. Proteome. Res. 10 (2011) 5070–5083.
[8] J.M. Llovet, J.Z. Rossi, E. Pikarsky, B. Sangro, M. Schwartz, M. Sherman, Hepatocellular carcinoma, Nat. Rev. Dis. Primers. 2 (2016) 16–18.
[9] B. Mannervik, P. Alin, C. Guthenberg, H. Jensson, M.K. Tahir, M. Warholm, H. Jörnvall, Identification of three classes of cytosolic glutathione transferase common to several mammalian species: correlation between structural data and enzymatic properties, Proc. Natl. Acad. Sci. U. S. A. 82 (1985) 7202–7206.
[10] D.J. Meyer, B. Coles, S.E. Pemble, K.S. Gilmore, G.M. Fraser, B. Ketter, Theta, a new class of glutathione transferases purified from rat and man, Biochem. J. 274 (1991) 409–414.
[11] T.M. Buetler, D.L. Eaton, Glutathione S-transferases: amino acid sequence comparison, classification and phylogenetic relationship, Environ. Carcinog. Ecotoxicol. Rev. 10 (1992) 181–203.
[12] D.J. Meyer, M.R. Thomas, Characterization of rat spleen prostaglandin H d-isomerase as a sigma-class GSH transferase, Biochem. J. 311 (1995) 739–742.
[13] S.E. Pemble, A.F. Wardle, J.B. Taylor, Glutathione S-transferase class Kappa: characterization by the cloning of rat mitochondrial GST and identification of a human homologue, Biochem. J. 319 (1996) 749–754.
[14] P.G. Board, R.T. Baker, G. Chelvanayagam, L.S. Jermiin, Zeta, a novel class of glutathione transferases in a range of species from plants to humans, Biochem. J. 328 (1997) 929–935.
[15] P.G. Board, M. Coggan, G. Chelvanayagam, S. Easteal, L.S. Jermiin, C.K. Schulte, D.E. Danley, L.R. Hoth, M.C. Griffor, A.V. Kamath, M.H. Rosner, B.A. Chrunyk, D.E. Perregaux, C.A. Gabel, K.F. Georghegan, J. Pandit, Identification, characterization, and crystal structure of the Omega class glutathione transferases, J. Biol. Chem. 275 (2000) 24798–24806.
[16] G. Ricci, F.D. Maria, G. Antonini, P. Turella, A. Bullo, L. Stella, G. Filomeni,

G. Federici, A.M. Caccuri, 7-Nitro-2,1,3-benzoxadiazole derivatives, a new class of suicide inhibitors for glutathione s-transferases, J. Biol. Chem. 280 (2005) 26397–26405.

[17] (a) D.J. Waxman, Glutathione s-transferases: role in alkylating agents resistance and possible target for modulation chemotherapy-A, Review. Cancer Res. 50 (1990) 6449–6454;
(b) B. Coles, B. Ketterer, The role of glutathione and glutathione transferases in chemical carcinogenesis, Crit. Rev. Biochem. Mol. Biol. 25 (1990) 47–70;
(c) D.M. Townsend, K.D. Tew, The role of glutathione-S-transferase in anti-cancer drug resistance, Oncogene 22 (2003) 7369–7375.

[18] K.D. Tew, A. Monks, L. Barone, D. Rosser, G. Akerman, J.A. Montali, J.B. Wheatley, D.E. Schmidt, Glutathione-associated enzymes in the human cell lines of the National Cancer Institute Drug Screening Program, Mol. Pharmacol. 50 (1996) 149–159.

[19] C.S. Thomas, S.L. Kelley, W.D. Henner, Identification of an anionic form of glutathione transferase present in many human tumors and human tumor cell lines, Cancer Res. 48 (1988) 527–533.

[20] J.D. Hayes, D.J. Pulford, The glutathione S-transferase supergene family: regulation of GST and the contribution of the isozymes to cancer chemoprotection and drug resistance, Crit. Rev. Biochem. Mol. Biol. 30 (1995) 445–600.

[21] A. Procopio, S. Alcaro, S. Cundari, A.D. Nino, F. Ortuso, P. Sacchetta, A. Pennelli, G. Sindona, Molecular modeling, synthesis, and preliminary biological evaluation of glutathione-S-transferase inhibitors as potential therapeutic agents, J. Med. Chem. 48 (2005) 6084–6089.

[22] Y. Soma, K. Satoh, K. Sato, Purification and subunit-structural and immunological characterization of five glutathione 5-transferases in human liver, and the acidic form as a hepatic tumor marker, Biochem. Biophys. Acta 869 (1986) 247–258.

[23] P. Sharma, J.P. Allison, The future of immune checkpoint therapy, Science 348 (2015) 56–61.

[24] S.L. Topalian, C.G. Drake, D.M. Pardoll, Immune checkpoint blockade: A common denominator approach to cancer therapy, Cancer Cell 27 (2015) 450–461.

[25] A.J. Muller, P.A. Scherle, Targeting the mechanisms of tumoral immune tolerance with small-molecule inhibitors, Nat. Rev. Cancer 6 (2006) 613–625.

[26] a) S.G. Awuah, Y.R. Zheng, P.M. Bruno, M.T. Hemann, S.J. Lippard, A Pt(IV) prodrug preferentially targets indoleamine-2,3-dioxygenase, providing enhanced ovarian cancer immunoChemotherapy, J. Am. Chem. Soc. 137 (2015) 14854–14857;
b) N. Wang, Z.G. Wang, Z.F. Xu, X.F. Chen, G.Y. Zhu, A cisplatin-loaded immunochemotherapeutic nanohybrid bearing immune checkpoint inhibitors for enhanced cervical cancer therapy, Angew. Chem. Int. Ed. 130 (2018) 3484–3488.

[27] J.S. Wu, S.Y. Lin, F.Y. Liao, W.C. Hsiao, L.C. Lee, Y.H. Peng, C.L. Hsieh, M.H. Wu, J.S. Song, A. Yueh, C.H. Chen, S.H. Yeh, C.Y. Liu, S.Y. Lin, T.K. Yeh, C. Shih, S.H. Ueng, M.S. Hung, S.Y. Wu, Identification of substituted naphthotriazolediones as novel tryptophan 2,3-dioxygenase (TDO) inhibitors through structure-based virtual screening, J. Med. Chem. 58 (2015) 7807–7819.

[28] E. Dolusic, P. Larrieu, L. Moineaux, V. Stroobant, L. Pilotte, D. Colau, L. Pochet, B.V. Eynde, B. Masereel, J. Wouters, R. Frederick, Tryptophan 2,3-dioxygenase (TDO) inhibitors. 3-(2-(Pyridyl)ethenyl) indoles as potential anticancer immunomodulators, J. Med. Chem. 54 (2011) 5320–5334.

[29] W.E. Knox, A.H. Mehler, The conversion of tryptophan to kynurenine in liver. I. The coupled tryptophan peroxidaseoxidase system forming formylkynurenine, J. Biol. Chem. 187 (1950) 419–430.

[30] a) C. Uyttenhove, L. Pilotte, I. Theate, V. Stroobant, D. Colau, N. Parmentier, T. Boon, B.J. Van den Eynde, Evidence for a tumoral immune resistance mechanism based on tryptophan degradation by indoleamine 2,3-dioxygenase, Nat. Med. 9 (2003) 1269–1274;
b) R. Meisel, A. Zibert, M. Laryea, U. Gçbel, W. D-ubener, D. Dilloo, Human bone marrow stromal cells inhibit allogeneic T-cell responses by indoleamine 2,3-dioxygenase-mediated tryptophan degradation, Blood 103 (2004) 4619–4621;
c) D.H. Munn, A.L. Mellor, Indoleamine 2,3-dioxygenase and tumor-induced tolerance, J. Clin. Invest. 117 (2007) 1147–1154.

[31] L. Pilottea, P. Larrieua, V. Stroobant, D. Colau, E. Dolušić, R. Frédérick, E.D. Plaen, C. Uyttenhove, J. Wouters, B. Masereel, B.J.V. Eyndea, Reversal of tumoral immune resistance by inhibition of tryptophan 2,3-dioxygenase, Proc. Natl. Acad. Sci. USA 109 (2012) 2497–2502.

[32] C.A. Opitz, U.M. Litzenburger, F. Sahm, M. Ott, I. Tritschler, S. Trump, T. Schumacher, L. Jestaedt, D. Schrenk, M. Weller, M. Jugold, G.J. Guillemin, C.L. Miller, I. Lehmann, A.V. Deimling, W. Wick, M. Platten, An endogenous tumour-promoting ligandof the human aryl hydrocarbon receptor, Nature 478 (2011) 197–203.

[33] H. Gao, K. Li, H. Tu, X. Pan, H. Jiang, B. Shi, Development of T cells redirected to glypican-3 for the treatment of hepatocellular carcinoma, Clin. Cancer Res. 20 (2014) 6418–6428.

[34] D.H. Palmer, R.S. Midgley, N. Mirza, E.E. Torr, F. Ahmed, J.C. Steele, A phase II study of adoptive immunotherapy using dendritic cells pulsed with tumour lysate in patients with hepatocellular carcinoma, Hepatology 49 (2008) 124–132.

[35] L.H. Butterfield, A. Ribas, V.B. Dissette, Y. Lee, J.Q. Yang, P.L. Rocha, A phase I/II trial testing immunization of hepatocellular carcinoma patients with dendritic cells pulsed with four alpha-fetoprotein peptides, Clin. Cancer Res. 12 (2006) 2817–2825.

[36] M. Lalle, S. Camerini, S. Cecchetti, R. Finelli, G. Sferra, J. Muller, G. Ricci, E. Pozio, The FAD-dependent glycerol-3-phosphate dehydrogenase of Giardia duodenalis: an unconventional enzyme that interacts with the g14-3-3 and it is a target of the antitumoral compound NBDHEX, Front. Microbiol. 6 (2015) 544.

[37] H.H. Sha, Z. Wang, S.C. Dong, T.M. Hu, S.W. Liu, J.Y. Zhang, Y. Wu, R. Ma, J.Y. Wu, D. Chen, J.F. Feng, 6-(7-nitro-2,1,3-benzoxadiazol-4-ylthio)hexanol: a promising new anticancer compound, Biosci. Rep. 38 (2018) 1–9.

[38] B. Shi, R. Stevenson, M.F. Greaney, Discovery of glutathione S-transferase inhibitors using dynamic combinatorial chemistry, J. Am. Chem. Soc. 128 (2006) 8459–8467.

[39] S.S. Zhang, S.P. Nie, D.F. Huang, Y.L. Feng, M.Y. Xie, A novel polysaccharide from ganoderma atrum exerts antitumor activity by activating mitochondria-mediated apoptotic pathway and boosting the immune system, J. Agric. Food Chem. 62 (2014) 1581–1589.

[40] F.J. Quintana, G. Murugaiyan, M.F. Farez, M. Mitsdoerffer, A.M. Tukpah, E.J. Burns, H.L. Weiner, An endogenous aryl hydrocarbon receptor ligand acts on dendritic cells and T cells to suppress experimental autoimmune encephalomyelitis, Proc. Natl. Acad. Sci. USA 107 (2010) 20768–20773.